

High numerical aperture microlens arrays of close packing

Dong Wu,¹ Si-Zhu Wu,¹ Li-Gang Niu,¹ Qi-Dai Chen,^{1,a)} Rui Wang,¹ Jun-Feng Song,¹ Hong-Hua Fang,¹ and Hong-Bo Sun^{1,2,a)}

¹State Key Laboratory on Integrated Optoelectronics, College of Electronic Science and Engineering, Jilin University, 2699 Qianjin Street, Changchun 130012, People's Republic of China

²College of Physics, Jilin University, 119 Jiefang Road, Changchun 130023, People's Republic of China

(Received 31 October 2009; accepted 19 June 2010; published online 20 July 2010)

Closed-packed high numerical aperture (NA) microlens arrays (MLA) are highly desirable for high resolution imaging and high signal-to-noise-ratio detection in micro-optical and integrated optical applications. However, realization of such devices remains technically challenging. Here, we report high quality fabrication of curved surfaces and MLAs by taking the full advantage of surface self-smoothing effect by creating highly reproducible voxels and by adopting an equal-arc scanning strategy. MLA of approximately 100% fill ratio and NA of 0.46, much greater than those ever reported, 0.13, is demonstrated, whose excellent optical performance was approved by the sharp focusing and high resolution imaging. © 2010 American Institute of Physics.

[doi:10.1063/1.3464979]

A microlens array (MLA), generally termed for a two-dimensional (2D) array of small lenses with diameters between micrometers and a millimeter, are widely used in integral photography, photocopying, facsimile, and high-speed parallel optical switching networks.¹⁻⁴ In order to reduce noise from the idle light that passes through lenslets intervals without focusing, and ensure high resolution and high signal-to-noise-ratio optical imaging and detection, MLAs of both high numerical aperture (NA) and high fill factor are continuously pursued. However, technical realization of such MLAs remains challenging despite massive efforts⁵⁻¹⁰ toward high fill factor⁵⁻⁷ and high NA.^{8,9} For example, the highest NA achieved from 100% fill factor MLAs produced by thermal reflow,^{5,7} multistep UV lithography,⁶ Ni-Co electroplating and hot embossing is solely 0.13; while the fill factor from high NA MLAs prepared by microfluidic technology⁸ and digital projection photopolymerization⁹ is lower than 50%.

Femtosecond laser direct writing technology has been known as a simple method to realize arbitrary geometry three-dimensional (3D) structures^{11,12} with a nanometric resolution. Typical fabrication examples include a microbull,¹³ a nano-oscillator,¹⁴ and photonic crystals.¹⁵ These complex 3D architectures were created with around 100 nm precision but they required less on the surface roughness.¹⁶ In contrast, for refractive optical components such as micropillar, concave micromirrors, and microlens, the surface roughness plays a critical role on their optical performance. Although Yang *et al.*¹⁷ and Huang *et al.*¹⁸ adopted thin layer slicing method to improve the surface quality of curved surfaces, it generally led to low fabrication efficiency. A systematic study is apparently needed to clarify the underlying physics of thin layer slicing, from which alternative high efficiency writing strategies, particularly on curved surfaces like an MLA, is expected. To reach this end, we report in this letter that highly reproducible voxels size and equal-arc slicing are critical to achieve high surface quality due to an effect we call self-

flattening, by which 100% fill factor MLAs of NA as large as 0.46, an upper limit set by the material refractive index is obtained.

Shown in Fig. 1(a) is a schematic surface written by two-photon polymerization, for which femtosecond laser beam of 800 nm wavelength and 120 fs pulsewidth, mode-locked at 82 MHz (from Tsunami, Spectra Physics) were tightly focused by a 100× objective with a NA of NA = 1.40, so as to induce polymerization in the focal spot.¹⁹ The power of the focus laser was adjusted around 6 mW. A two-galvano-mirror set along with a one-dimensional piezo stage where located the sample made the focal spot move three dimensionally relative to the sample resist of SU-8, which had been coated on a cleaned glass substrate and treated in a standard procedure recommended by MicroChem (the manufacturer of SU-8). The laser written structures were rinsed in the developer so that unpolymerized photoresist could be removed, leaving the expected device structures. According to our previous study¹⁶ small protrusions in a photopolymerized surface tend to be straightened by local surface tension occurring in the course of unpolymerized resin rinsing, an

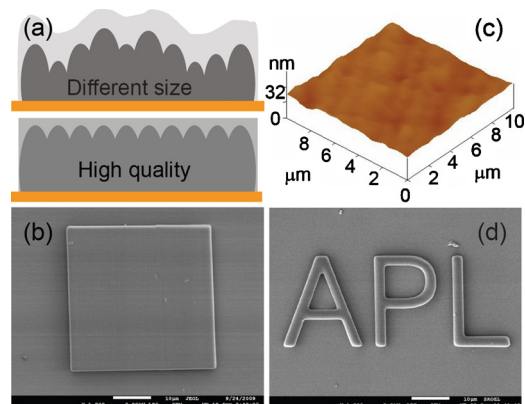


FIG. 1. (Color online) High surface smoothness realized by high reproducibility control of voxels. (a) Self-smoothing effect arising from surface tension. (b) A $10 \times 10 \mu\text{m}^2$ square fabricated by this improved femtosecond technology. (c) The AFM image showing high surface smoothness. (d) Three microletters "APL" with high surface quality.

^{a)}Authors to whom correspondence should be addressed. Electronic addresses: chenqd@jlu.edu.cn and hbsun@jlu.edu.cn.

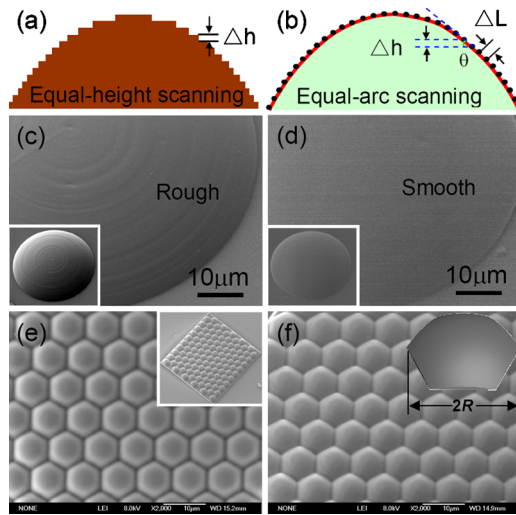


FIG. 2. (Color online) Curved surface fabrication. (a) Equal-height scanning mode. (b) Equal-arc scanning mode. (c) and (d) SEM images of single microlens prepared by the two scanning methods. (e) Top-view SEM images of the gapless hexagonal microlens arrays. The inset is the whole tiled-view SEM image. There is no gap between two adjacent lenses. (f) 35° tilted-view locally magnified image. The inset is the solid model of a hexagonal microlens.

effect here we call self-smoothing effect. However, it has been experimentally observed that the fluctuation of the voxels size is the major factor that counteracts the self-smoothing effect even if the scanning step is sufficiently small [the upper image of Fig. 1(a)]. This is associated with the quadratic dependence of photopolymerization rate on the laser light intensity. Slight variation in laser pulse energy may induce significant surface protrusion or pits. In order to solve this problem, series of measures are taken to stabilize the laser pulse energy including maintaining the local temperature around the laser within 23 ± 0.2 °C and an output feedback system was equipped so that the laser pulse energy fluctuation was lowered to less than 0.5%. Under this circumstance, the self-smoothing effect starts to play an essential role in determining the overall surface quality [the lower image of Fig. 1(a)]. Surface roughness defined by the root of mean square on 10×10 μm^2 planar squares were less than 2.5 nm for voxel-voxel distance of 100 nm [Figs. 1(b) and 1(c)], far better than results so far achieved. With the strategy, microletters “APL” [Fig. 1(d)] was written, showing the high surface quality.

For 3D curved microstructures like typical lens structures, the slicing layer thickness is another determinant factor for high surface quality. Shown in Fig. 2(c) is the typical scanning electron microscopic (SEM) image of a lens surface attained with equal-height slicing [Fig. 2(a)] and the vertical step is standard $\Delta h = 100$ nm. The significant solenoid traces were caused by the lateral offset of voxels location, which is beyond the capability that is able to be flattened by the self-smoothing effect. In order to compensate the large inward shift in voxels layer by layer, from the bottom to the top, we adopt an equal-arc scanning strategy [Fig. 2(b)], whereby the distance between adjacent voxels keeps constant and the layer height $\Delta h = \Delta L \times \sin \theta$ becomes a variant, depending on the arc length ΔL and the sloping angle θ . With ΔL chosen the same as the case of planar scanning, 100 nm, high quality curved surfaces were attained [Fig. 2(d)]. It takes solely 6 min to complete a microlens structure of

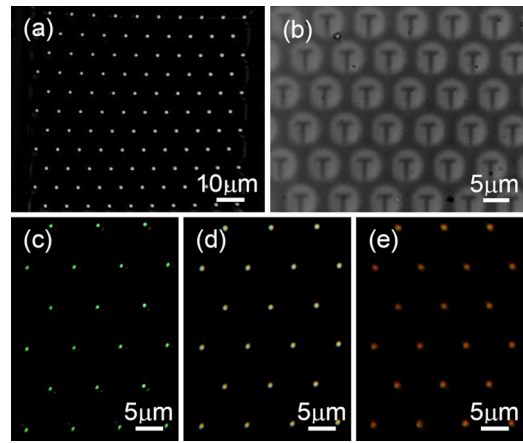


FIG. 3. (Color online) Sharp focusing characteristics of high MLAs. (a) The observed focal spot arrays. (b) A hexagonal array of miniaturized “T” letters on the focal plane of the HMLAs illuminated by halogen lamp. [(c)–(e)] Photographs of foci with different colors at the different focal plane such as green, yellow, and red focal spot arrays.

$\phi = 80$ μm , where ϕ is the base diameter, provided that only the lens surface layer, a nanoshell, is depicted by means of two-photon photopolymerization¹⁶ while the inner portion is solidified by UV irradiation [Fig. 2(d)].

Aided with the self-smoothing and equal-arc depicting technologies, MLAs consisting of curved surfaces are prepared with high-efficiency and high accuracy. For close packed geometry, lenslets should be edge-cut considering 2D rotation symmetry of the repetitive primitive unit. Among various patterns with C_3 (triangle), C_4 (square), or C_6 (hexagon) axis,²⁰ hexagonally cutting was chosen because of the most proximity of a hexagon to a circle, through which the off-axis deviation of the entire incident light and therefore the spherical aberration in imaging were minimized. Experimentally, inscribed hexagons of 10 μm diameter and 1.5 μm height were prepared in close-packed way [Figs. 2(e) and 2(f)]. It takes about 4 min to prepare the hexagonal MLA with 90 μm outer diameter and 300 nm nanoshell thickness, against 30 min if the entire structures were solidified by two-photon process.

In order to investigate optical properties of the high fill-factor MLAs, they were characterized with the optical setup comprising a 3D positioning stage, an objective lens, a halogen lamp and a charged coupled devices camera. A hexagonal array of bright focal spots was observed behind the microscopic objective lens [Fig. 3(a)]. The brightness and size of the focal spots are quite uniform. The focal length of lenslets is estimated according to $f = (R^2 + h^2) / 2h(n-1) - h(n-1)$, where R and n are the radius of the lenslets and the refractive index of SU-8, respectively. Given $R = 5$ μm , $h = 1.5$ μm , and $n = 1.5858$, we have $f = 14.6$ μm , agreeing with the measured value of 14 μm . With these date, the f -number of the lenslets in the array, defined by $N = f/D$, where f is the focal length and D is the diameter of the entrance pupil, is estimated to be around 1.4. Such low values of f and N are within the expectation because the small diameters of microlenses impose small value for radius of curvature and small amount of light was collected. Considering materials dispersion, the lens focal length is actually sensitive to wavelength, and light of different colors are not focused to the same focal plane in a high quality single lens, which is known as longitudinal chromatic aberration or axial

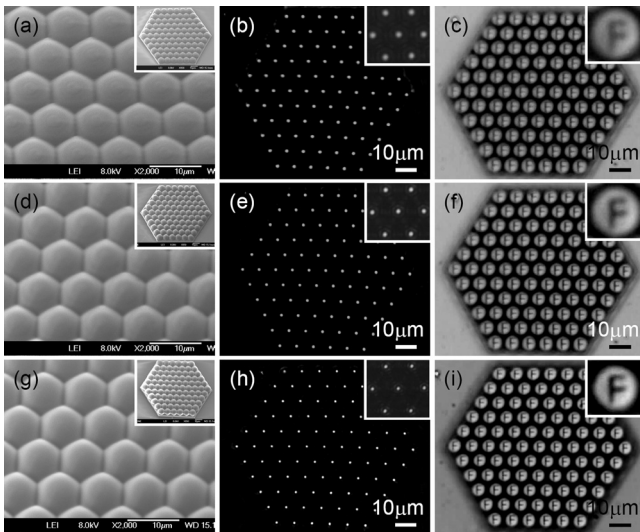


FIG. 4. High quality microlens arrays with designable NAs. (a), (d), and (g) Titled-view SEM images of gapless HMLAs with the same size and different heights. The heights of microlens are $1.2 \mu\text{m}$, $1.8 \mu\text{m}$, and $2.4 \mu\text{m}$, respectively. The insets are their whole SEM images. (b), (e), and (h) are their focal spots. (c), (f), and (i) are their arrays of miniaturized “F” images. The six insets are the locally magnified images which showed higher resolution and clearer imaging realized by these high quality HMLAs.

color. Axis color is generally difficult to be observed in a microlens and it is detrimental for high quality imaging. However, its appearance could be a useful criterion showing the high quality of microlens fabrication, as shown by the green [Fig. 3(c)], yellow [Fig. 3(d)], and red [Fig. 3(e)] focal planes.

An important factor that determines the imaging quality of MLAs is resolution, a function of NA, roughly defined as $NA=R/\sqrt{R^2+f^2}$, meaning that NA is designable by its geometrical parameters. Shown in Fig. 4 are hexagonal arrays of microlenses with NAs of 0.27, 0.38, and 0.46, deduced from the lens radius of $R=5 \mu\text{m}$ and the heights of $h=1.2 \mu\text{m}$ [Fig. 4(a)], $1.8 \mu\text{m}$ [Fig. 4(d)], and $2.4 \mu\text{m}$ [Fig. 4(g)], respectively. The NA value is much larger than those ever reported,⁷ 0.13. Further increase in the height leads to the total reflection when light propagates out of the lens with a parabolic surface profile, implying that $NA=0.46$ has approached the upper limit set by the material. Assumed diffraction limited focusing, the diameters of the focal spots calculated by Rayleigh criterion, $D=1.22 \lambda/NA$, for $\lambda=632.8 \text{ nm}$ are $2.86 \mu\text{m}$, $2.03 \mu\text{m}$, and $1.68 \mu\text{m}$, for lenslets of $NA=0.27$, 0.38, and 0.46, respectively. This is consistent with the tendency of focal spot size variation exhibited from Figs. 3(b), 3(e), and 3(h). The smallest size [Fig. 4(h)] of the focal spot was about $1.5 \mu\text{m}$, much smaller than the value ($\sim 8 \mu\text{m}$) ever reported.⁶ This, together with the gradually sharper contrast of the image of a letter “F” from the top to the bottom in Fig. 4, provides further proof of the optical quality of the microlens. It is worthy to mention that

the high quality imaging should be associated with the fact that the surface profiles of lenslets are not spherical but parabolic.²¹ In another word, the MLA consists of aspherical microlenses, through which, the spherical aberration has been minimized.

In conclusion, MLAs consisting of closed-packed, high NA and aspheric profiles have been fabricated by an improved femtosecond induced two-photon photopolymerization technology. The high surface quality of the lens was ensured by the highly reproducible voxels and their arrangement in equal-arc scanning strategy, which take the full advantage of self-smoothing effect. The diffraction-limit focusing capability and high contrast imaging was experimentally demonstrated, showing the vast potential applications of the devices on, for example, beam shaping, optical interconnection, and integrated optical systems.

This work was supported by NSFC (Grant Nos. 90923037, 60525412, and 60778004).

- ¹C. Berger, N. Collings, R. Volkel, M. T. Gale, and T. Hessler, *Pure Appl. Opt.* **6**, 683 (1997).
- ²Y. Huang, D. Shieh, and S. Wu, *Appl. Opt.* **43**, 3656 (2004).
- ³J. Lim, S. S. Oh, D. Y. Kim, S. H. Cho, I. T. Kim, S. H. Han, H. Takezoe, E. H. Choi, G. S. Cho, Y. H. Seo, S. O. Kang, and B. Park, *Opt. Express* **14**, 6564 (2006).
- ⁴L. Erdmann and K. J. Gabriel, *Appl. Opt.* **40**, 5592 (2001).
- ⁵C. P. Lin, H. Yang, and C. K. Chao, *J. Micromech. Microeng.* **13**, 775 (2003).
- ⁶M. C. Chou, C. T. Pan, S. C. Shen, M. F. Chen, K. L. Lin, and S. T. Wu, *Sens. Actuators, A* **118**, 298 (2005).
- ⁷S. Y. Hung, C. K. Chao, T. H. Lin, and C. P. Lin, *J. Micromech. Microeng.* **15**, 2389 (2005).
- ⁸A. Tripathi, T. V. Chokshi, and N. Chronis, *Opt. Express* **17**, 19908 (2009).
- ⁹Y. Lu and S. Chen, *Appl. Phys. Lett.* **92**, 041109 (2008).
- ¹⁰W. L. Chang and P. K. Wei, *Opt. Express* **15**, 6774 (2007).
- ¹¹D. Wu, Q. D. Chen, L. G. Niu, J. N. Wang, R. Wang, H. Xia, and H. B. Sun, *Lab Chip* **9**, 2391 (2009).
- ¹²D. Wu, L. G. Niu, Q. D. Chen, R. Wang, and H. B. Sun, *Opt. Lett.* **33**, 2913 (2008).
- ¹³S. Kawata, H.-B. Sun, T. Tanaka, and K. Takada, *Nature (London)* **412**, 697 (2001).
- ¹⁴H. Xia, J. Wang, Y. Tian, Q. D. Chen, X. B. Du, Y. L. Zhang, Y. He, and H. B. Sun, “Ferrofluids for fabrication of remotely controllable micro-nanomachines by two-photon polymerization,” *Adv. Mater. (Weinheim, Ger.)* (to be published), DOI: 10.1002/adma.20100542.
- ¹⁵K. K. Seet, V. Mizeikis, S. Matsuo, S. Juodkazis, and H. Misawa, *Adv. Mater. (Weinheim, Ger.)* **17**, 541 (2005).
- ¹⁶K. Takada, H. B. Sun, and S. Kawata, *Appl. Phys. Lett.* **86**, 071122 (2005).
- ¹⁷S. H. Park, S. H. Lee, D. Y. Yang, H. J. Kong, and K. S. Lee, *Appl. Phys. Lett.* **87**, 154108 (2005).
- ¹⁸R. Guo, S. Z. Xiao, X. M. Zhai, J. W. Li, A. D. Xia, and W. H. Huang, *Opt. Express* **14**, 810 (2006).
- ¹⁹H. B. Sun, T. Suwa, K. Takada, R. P. Zaccaria, M. S. Kim, K. S. Lee, and S. Kawata, *Appl. Phys. Lett.* **85**, 3708 (2004).
- ²⁰C. T. Pan and C. H. Su, *Sens. Actuators, A* **134**, 631 (2007).
- ²¹D. Wu, Q. D. Chen, L. G. Niu, J. Jiao, H. Xia, J. F. Song, and H. B. Sun, *IEEE Photonics Technol. Lett.* **21**, 1535 (2009).